

Computation of Internal Flows: Methods and Applications

presented at

ENERGY SOURCES TECHNOLOGY CONFERENCE
NEW ORLEANS, LOUISIANA
FEBRUARY 12-16, 1984

sponsored by

THE FLUID MACHINERY AND FLUID MECHANICS COMMITTEES
FLUIDS ENGINEERING DIVISION, ASME

edited by

PETER M. SOCKOL
NASA LEWIS RESEARCH CENTER

KIRTI N. GHIA
UNIVERSITY OF CINCINNATI

8. Lecomte, C., "Calculation of Cascade Profiles from the Velocity Distribution," ASME Paper No. 74-GT-70.

9. Lewis, R. I., "A Method for Inverse Design Aerofoils and Cascade Design by Surface Vorticity," ASME Paper No. 82-GT-154.

10. Kashiwabara, Y., "Theory on Blades of Axial, Mixed, and Radial Turbomachines by Inverse Method," Bulletin of the JSME, February 1973.

11. Wu, C. H., and Brown, C. A., "A Theory of the Direct and Inverse Problems of Compressible Flow Past Cascade of Arbitrary Airfoils," Journal of Aero. Science, March 1952.

12. Novak, R. A., and Haymann-Haber, G., "A Mixed-Flow Cascade Passage Design Procedure Based on a Power Series Expansion," ASME Paper No. 82-GT-121.

13. McFarland, E. R., "Solution of Plane Cascade Flow Using Improved Surface Singularity Methods," NASA TM 81589, March 1981.

DETERMINATION OF THE AXISYMMETRIC
POTENTIAL FLOW IN THE PASSAGES
OF TURBOMACHINES USING THE
METHOD OF SINGULARITIES

Alexander Gokhman
Senior Staff Engineer

Research and Development Division
Allis-Chalmers Fluid Products Company
York, Pennsylvania

ABSTRACT

This paper presents the application of the method of singularities to the problem of axisymmetric flow in fluid passages, and utilizes newly developed numerical techniques to achieve a highly accurate solution. In the proposed method the fluid passages are considered to be infinite at both entrance and exit. For example, in the case of a Francis turbine, the fluid passage at the entrance go to infinity between two planes perpendicular to the turbine axis and at the exit, go to infinity inside of the cylinder parallel to the turbine axis. The γ -distribution along the infinite surfaces of revolution is determined as a solution of a Fredholm integral equation of the second kind.

NOMENCLATURE

r, z and θ cylindrical coordinates (the positive direction for z -axis is downstream).
 \vec{V} the flow velocity vector.
 V_r, V_z and V_θ radial, axial and circumferential flow velocity projections.
 γ the intensity of distributed vorticity along the surfaces bounding the fluid passages (γ is positive in clockwise direction).
 Q volume flow rate
 b_o the height of the radial inlet/exit, Fig. 1.
 r_{co} and r_{ci} the radii of the outer and inner cylinders of an axial inlet/exit, Fig. 1.

Φ the velocity potential.
 \hat{n} the unit vector normal to the surfaces of revolution bounding the fluid passages (directed towards the inside of the passages).
 l the length along a meridional line forming the bounding surface of revolution.

INTRODUCTION

The method of singularities gave excellent results when applied to the analysis and synthesis problems for two-dimensional cascades of hydrofoils [1, 2, 3, 4]. To the best of the author's knowledge, this method has never been applied to the determination of the axisymmetric potential flow in the passages of turbomachines.

In the majority of recent works, the axisymmetric flow in the fluid passages was determined using streamline curvature method, finite differences or finite elements [5, 6, 7, 8]. However, the application of these methods to this problem can lead to undesirably high values of relative error in the velocity field determination. These errors can approach the level of about 4% [5, 8]. In contrast, the first attempt of applying the method of singularities (which is described in the present paper), to the velocity field determination in the passages of turbomachines produced a solution of very high accuracy with a maximum relative error equal to 0.4%.

The proposed solution can be applied only to fluid passages having the following types of geometrical boundaries:

1. Radial Inlet/Exit

The passage is formed by two planes perpendicular to the axis of symmetry (axis of turbomachine), and extend to infinity.

2. Axial Inlet/Exit

The passage is formed by an axial annulus along the axis of symmetry and extend to infinity (the absence of an inner cylinder is a special case of this type).

It is clear that the fluid passages under consideration include all practical cases (for axisymmetric flow) used in turbomachinery (Fig. 1 shows a representative sketch of a Francis hydro-turbine having this type of passage).

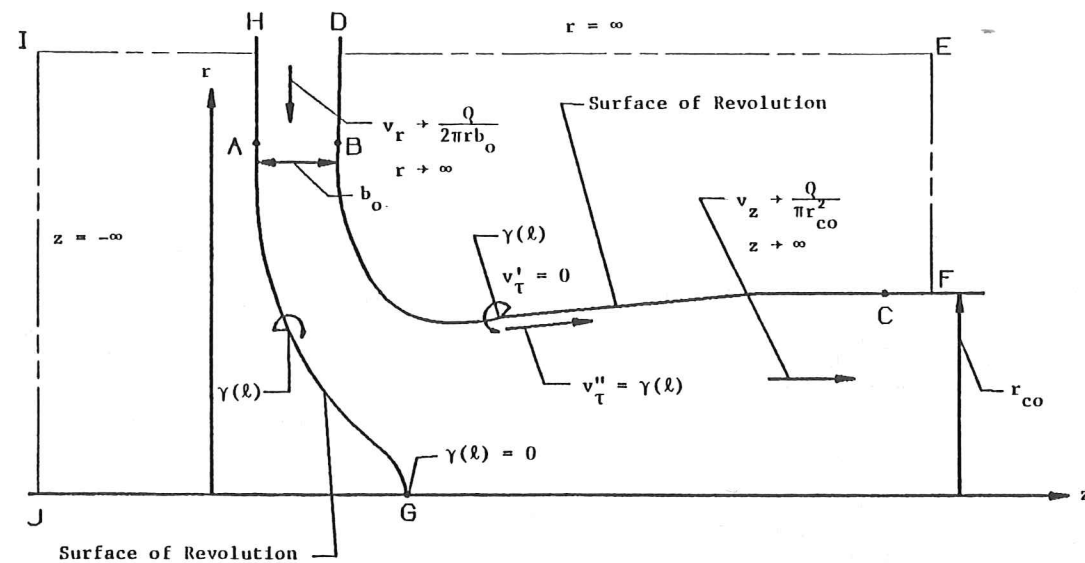


Fig. 1 The sketch of a Francis hydro-turbine fluid passage

FORMULATION OF THE PROBLEM

Assumptions

- * Fluid is inviscid and incompressible.
- ** Flow is potential and axisymmetric
- *** The circumferential projection of the flow velocity is zero.

Governing Equation

The flow of fluid satisfying the accepted assumptions is described by Laplace's Equation [9]:

$$\frac{\partial^2 \phi}{\partial z^2} + \frac{1}{r} \frac{\partial \phi}{\partial r} + \frac{\partial^2 \phi}{\partial r^2} = 0 \quad (1)$$

and the velocity projections are expressed using potential by the following formulae:

$$V_z = \frac{\partial \phi}{\partial z} \quad (2)$$

$$V_r = \frac{\partial \phi}{\partial r} \quad (3)$$

Boundary Conditions

* Radial Inlet/Exit

At infinity ($r \rightarrow \infty$) the flow is uniform, radial and $V_r \rightarrow 0$; therefore, the boundary conditions have the following form:

$$\lim_{r \rightarrow \infty} \frac{V_r}{\frac{Q}{2\pi b_o r}} = \pm 1 \quad (4)$$

The plus sign in (6) and (7) corresponds to the inlet and the minus to the exit.

*** The Surfaces of Revolution Which Bound the Fluid Passages

At each point on these surfaces:

$$V_n = 0 \quad (8)$$

or

$$(\vec{V} \cdot \hat{n}) = 0$$

The expression for an inside normal \hat{n} , in the case of a meridional line ($r = r(\ell)$, $z = z(\ell)$) forming the surface of revolution is given by the following formula:

$$\hat{n} = \pm \left(\frac{dz}{d\ell} \hat{e}_r - \frac{dr}{d\ell} \hat{e}_z \right) \quad (9)$$

where the plus sign is for the inner surface and the minus sign is for the outer surface.

Therefore, the boundary conditions described in (8) can be rewritten in the form:

$$V_r \frac{dz}{d\ell} - V_z \frac{dr}{d\ell} = 0 \quad (10)$$

THEORY AND METHODOLOGY

In order to generate the potential axisymmetric flow inside the fluid passages, the bounding surfaces of revolution are covered with distributed circular vortex filaments of intensity $\gamma(\ell)$ (ℓ is the length along meridional line forming the surface of revolution).

There are several conditions the γ -distribution has to satisfy. These conditions evidently depend on the type of turbomachine under consideration. In Francis and Kaplan hydro-turbines, for example, the radial-axial fluid passage shown on Figure 1 has to be considered and γ -distribution has to satisfy the following conditions which are known a priori to the solution.

* Along two radial planes forming the intake:

$$\lim_{r \rightarrow \infty} \frac{\gamma(r)}{\frac{Q}{2\pi b_o r}} = \pm 1 \quad (11)$$

$r \rightarrow \infty$

where + is for upstream plane and - is for downstream plane

** Along the cylinder forming the discharge:

$$\lim_{z \rightarrow \infty} \gamma(z) = -\frac{Q}{\pi r_c^2} \quad (12)$$

$z \rightarrow \infty$

*** At the point of intersection of the inner bounding surface with the axis of turbomachine:

$$\gamma = 0 \quad (13)$$

The conditions (11) and (12) are imposed in order to generate the flow which satisfies the boundary conditions (4), (5), (6) and (7). This immediately follows from the results obtained for vortices distributed along two semi-infinite radial planes and for vortices distributed along the semi-infinite cylinder (see Appendix 1). The condition (13) follows from the continuity of the velocity field in the fluid passages.

For the other type of turbomachine the conditions similar to (11), (12) and (13) can be easily established. It is clear that all practical cases for these conditions have to be incorporated in the subsequent computer program.

The values of $\gamma(\ell)$ at all other points of inner and outer bounding surfaces are unknown and have to be established as a result of the solution.

Change of Boundary Conditions along the Bounding Surfaces

It is well known that the boundary condition (8) along the surfaces bounding the fluid passages leads to a Fredholm equation of the first kind which is not suitable for the determination of γ -distribution, since in this case it can produce high inaccuracies and even an erroneous solution [1,10]. In order to apply the Fredholm equation of the second kind to our problem the boundary condition (8) has to be changed to the equivalent condition:

$$V_t^1 = 0 \quad (14)$$

where V_t^1 is the velocity component tangent to the bounding surface outside the fluid passages.

The proof of equivalency of the conditions (14) and (8) follows [10].

Suppose we found a γ -distribution which satisfies conditions (11), (12) and (14). Let us consider the domain formed by the bounding surface meridional line DF and two straight lines (see Figure 1):

$$r = r_M \quad (\text{line DE})$$

$$z = z_M \quad (\text{line EF})$$

It is easy to show that velocity induced by the vortices along these lines V_M (along DE) and V_N (along EF) satisfies the following conditions:

$$\lim V_M = 0 \quad (15)$$

$$\lim_{r_M \rightarrow \infty} V_M = 0 \quad (16)$$

$$\lim_{z_N \rightarrow \infty} V_N = 0$$

If one takes points A and B (on straight lines forming the radial part of the intake) and point C (on a straight line forming the cylindrical part of discharge), then the vortices distributed between

points A and G, and points B and C cover two finite surfaces of revolution and the velocity V_F induced at the point (r_c, z_c) by these vortices satisfies the following conditions:

$$\lim_{V_F} = 0 \quad (17)$$

$$r_c \rightarrow \infty (z_c = \text{const})$$

$$\lim_{V_F} = 0 \quad (18)$$

$$z_c \rightarrow \infty (r_c = \text{const})$$

It also follows from Appendix 1 that velocity along the lines DE and EF induced by the vortices distributed along two radial semi-infinite planes ($z = z_B$, $r_B \leq r < \infty$ and $z = z_A$, $r_A \leq r < \infty$) and by semi-infinite cylinder ($r = r_{co}$, $z_F \leq z < \infty$) goes to zero when $r_M \rightarrow \infty$ and $z_N \rightarrow \infty$. Therefore, we proved the conditions (15) and (16). Now it is clear that $V_t = 0$ along the closed contour BDEFCA (along the line FCBD one considers the points outside the fluid passages).

Let us consider the volume T_s bounded by the surface of revolution A_s formed by rotation of contour BDEFCA around the axis. Since there are no vortices inside volume T_s , the flow inside T_s is potential and:

$$\frac{\partial \phi}{\partial t} = V_t = 0 \quad (17)$$

or

$$\phi_s = \text{const} \quad (18)$$

where ϕ_s is the potential along contour BDEFCA.

It is easy now to show that there is a stagnation zone inside the surface A_s . Indeed, in application to the volume T_s , Green's formula [12] gives:

$$\iint_{T_s} (\nabla^2 \phi + \nabla \phi \cdot \nabla \phi) dT_s = \iint_{A_s} \phi \frac{\partial \phi}{\partial n} dA_s \quad (19)$$

where ϕ is the potential inside the volume T_s .

On the other hand since there are no sources/sinks inside volume T_c the conservation of mass provides that:

$$\iint_{A_s} \frac{\partial \phi}{\partial n} dA_s = 0 \quad (20)$$

Also since ϕ is the velocity potential:

$$\nabla^2 \phi = 0 \quad (21)$$

Now substituting (18), (20) and (21) into (19) one obtains that:

$$\iint_{T_s} (\nabla \phi \cdot \nabla \phi) dT_s = 0 \quad (22)$$

and since $\nabla \phi \cdot \nabla \phi \geq 0$ and $dT_s > 0$ it follows from (22) that at every point of T_s :

$$\nabla \phi \cdot \nabla \phi = 0$$

or

$$\nabla \phi = 0 \quad (23)$$

The equation (23) proves that volume T_s is the stagnation zone. Therefore, the normal component of velocity at each point along the line FCBD outside the water passages is equal to zero and, since the normal component is continuous for the vortex sheet, the boundary condition (8) is satisfied. Of course it is clear that the same is true for contour GAH.

It is also easy to see that condition (14) is equivalent to the condition:

$$V_t^{11} = \gamma \quad (24)$$

where V_t^{11} is the velocity component tangent to the bounding surface inside the fluid passages

The condition (24) directly follows from (14) and from the fact that for the axisymmetric vortex sheet [10]:

$$V_t^{11} - V_t^1 = \gamma \quad (25)$$

Integral Equation for Determination of γ -Distribution

The integral equation for γ determination directly follows from condition (14). If V_t^1 and V_t^{11} at the point (r_c, z_c) of bounding surface are introduced, as:

$$V_t^1 = V_t - \frac{\gamma(\ell_c)}{2} \quad (26)$$

$$V_t^{11} = V_t + \frac{\gamma(\ell_c)}{2} \quad (27)$$

where V_t is the tangential component of velocity induced by all vortex circular filaments $\gamma(\ell)$ distributed along the bounding surface excluding the filaments passing along the infinitesimal segment containing point $\ell_c = \ell(r_c, z_c)$

and tangential unit vector at point (r_c, z_c) is:

$$\hat{t} = \frac{dr}{d\ell} \Big|_{r_c, z_c} \hat{e}_r + \frac{dz}{d\ell} \Big|_{r_c, z_c} \hat{e}_z \quad (28)$$

then the integral equation can be written, as:

$$\gamma(\ell_c) = 2 [V_r(r_c, z_c) \frac{dr}{d\ell} \Big|_{r_c, z_c} + V_z(r_c, z_c) \frac{dz}{d\ell} \Big|_{r_c, z_c}] \quad (29)$$

The velocity components in (29) can be expressed (using formulae (69) and (70) of Appendix 1) as:

$$V_r(r_c, z_c) = - \int_{L_s} \int_0^{2\pi} \frac{\gamma(\ell)(z_c - z) \sin \theta r d\theta d\ell}{4\pi[R(r, z, \theta)]^{1.5}} \quad (30)$$

$$V_z(r_c, z_c) = - \int_{L_s} \int_0^{2\pi} \frac{\gamma(\ell)(r - r_c \sin \theta) r d\theta d\ell}{4\pi[R(r, z, \theta)]^{1.5}} \quad (31)$$

where

$$R(r, z, \theta) = r_c^2 - 2rr_c \sin \theta + r^2 + (z - z_c)^2$$

and

L_s is the contour including two infinite meridional lines forming the bounding surfaces of revolution (Figure 1).

The equations (29), (30) and (31) constitute the Fredholm equation of the second kind, which generally can be solved only numerically.

NUMERICAL SOLUTION

For the practical numerical solution it was accepted that γ is equal to its asymptotic value along the semi-infinite lines of boundary.

Therefore for the fluid passages shown in Figure 1:

Along the lines forming the radial intake (+ is for the line AH, - is for the line BD):

$$\gamma(r) = \pm \frac{Q}{2\pi b_0 r} (r_A \leq r < \infty) \quad (32)$$

Along the line CF forming the axial discharge:

$$\gamma(z) = - \frac{Q}{\pi r_{co}^2} (z_c \leq z < \infty) \quad (33)$$

It can be shown that the value of normal velocity at points A, B and C can be made of any desirable small value by accepting sufficiently large values for r_A and z_c .

For the finite parts of the meridional lines (in Figure 1 lines GA and CB) γ -distribution is unknown and has to be determined using the integral equation (29).

Each finite part is divided into certain number of segments and along each i -segment γ is represented either by a Hermite interpolant polynomial or by a linear function. In the case of Hermite interpolant polynomials the entire γ -distribution forms a continuous function of ℓ with continuous derivative $\frac{d\gamma}{d\ell}$ at each point. In the case of a linear function the γ -distribution forms a polygonal function with $\frac{d\gamma}{d\ell}$ constant along each segment and discontinuous at the end points of the segments.

Polygonal γ -Distribution

In this case γ is represented along each segment i by the following formula:

$$\gamma^i(\ell) = \gamma_i(1-\lambda) + \gamma_{i+1}\lambda \quad [1 \leq i \leq N-1] \quad (34)$$

where

$$\lambda = \frac{\ell - \ell_i}{\Delta \ell_i} \quad [0 \leq \lambda \leq 1]$$

$$\Delta \ell_i = \ell_{i+1} - \ell_i$$

The values of γ at the end points (γ_i and γ_{i+1}) in (34) are unknown and have to be determined. If the solution of the integral equation (29) is sought using (34), the point r_{cj}, z_{cj} on each segment at which the value of γ is being evaluated has to be inside the segment (since at the end points of segments $\frac{d\gamma}{d\ell}$ is discontinuous). The most convenient from a computational point of view is the point r_{cj}, z_{cj} which is the midpoint of each segment and in this case the integral equation (29) is reduced to the system of $N-2$ linear algebraic equations with $N-2$ unknown values of γ_j (for $N-1$ segments only $N-2$ values of γ_j are unknown since γ_1 and γ_N are defined by (32) and (33)):

$$0.5 (\gamma_j + \gamma_{j+1}) = (V_{rt} \frac{dr}{d\ell} + V_{zt} \frac{dz}{d\ell})_{r_{cj}, z_{cj}} + \sum_{i=1}^{N-1} \sum_{k=0}^1 [(V_{r,i+k,j})_{\ell} \frac{dr}{d\ell} \Big|_{r_{cj}, z_{cj}} + (V_{z,i+k,j})_{\ell} \frac{dz}{d\ell} \Big|_{r_{cj}, z_{cj}}] \gamma_{i+k} \quad (35)$$

($j=1, \dots, N-2$)

where $(V_{rt})_{r_{cj}, z_{cj}}$ and $(V_{zt})_{r_{cj}, z_{cj}}$ are velocity components induced by γ distributed along semi-infinite straight lines (formulae (32) and (33)) at the point (r_{cj}, z_{cj}) .

$(V_{r,i+k,j})_{\ell}$ and $(V_{z,i+k,j})_{\ell}$ are the influence functions of γ_{i+k} at the middle point of segment j (these functions are obtained by integration in Appendix 2).

The system (35) can be solved by various methods (Gauss elimination, etc). In the present paper this system is solved by the method of iterations using the fact that the values of influence functions $(V_{r,i+k,j})_{\ell}$ and $(V_{z,i+k,j})_{\ell}$ are much smaller by absolute value than 0.5. Therefore, for the first iteration the following formulae are used:

$$\gamma_{j,av} = (V_{rt} \frac{dr}{d\ell} + V_{zt} \frac{dz}{d\ell})_{r_{cj}, z_{cj}} \quad (36)$$

$$j=1, \dots, N-2$$

where

$$\gamma_{j,av} = 0.5 (\gamma_j + \gamma_{j+1}) \quad (37)$$

The values of γ_j for $j=2, \dots, N-1$ can be found from (37) by a simple rearrangement (note that γ_1 is known):

$$Y_{j+1} = Y_{j,av} - Y_j \quad (j=1, N-2)$$

For the subsequent iterations the entire formula (35) is used and the values of Y_j obtained by means of previous iteration are employed in the evaluation of the right hand side of the formula (35). The iterations converge very rapidly and provide any desirable accuracy of the solution of system (35). When values of Y_j ($j=2, \dots, N-1$) are determined the velocity components at any point inside the fluid passages can be computed. For the points located on the boundary the biggest error of computation occurs evidently at the end points of the segments j , since these points are the points of discontinuity for $\frac{dY}{d\ell}$.

Smooth γ -Distribution

For this case γ is represented by a Hermite interpolant polynomial [11] along each segment i :

$$Y^i(\ell) = Y_{i10} H_{10} + Y_{i20} H_{20} + \Delta \ell_i \left(\frac{dY}{d\ell} \Big|_{i11} H_{11} + \frac{dY}{d\ell} \Big|_{i21} H_{21} \right) \quad (38)$$

where $H_{10} = 1 - 3\lambda^2 + 2\lambda^3$

$$H_{20} = 3\lambda^2 - 2\lambda^3$$

$$H_{11} = \lambda - 2\lambda^2 + \lambda^3$$

$$H_{21} = \lambda^3 - \lambda^2$$

and $\lambda = \frac{\ell - \ell_i}{\Delta \ell_i} \quad [0 \leq \lambda \leq 1]$

If the solution is sought using (38) then there are N additional unknown $\frac{dY}{d\ell} \Big|_j$ ($j=1, \dots, N$). In order to determine these additional unknowns one can use the method of iterations. For the first iteration the linear formula (34) is applied and the values of Y_j ($j=2, \dots, N-1$) are determined. Then the splining technique is applied to $\gamma(\ell)$ defined by N values of Y at the end points of segments and the values of $\frac{dY}{d\ell} \Big|_j$ ($j=1, \dots, N$) are found [11].

For the computation of subsequent iterations the following equation is used instead of (35):

$$Y_{j,av} = \left(v_{rt} \frac{dr}{d\ell} + v_{zt} \frac{dz}{d\ell} \right)_{r_{cj}, z_{cj}} + \sum_{i=1}^{N-1} \sum_{k=0}^1 \left[(v_{r,i+k,j})_s \frac{dr}{d\ell} \Big|_{r_{cj}, z_{cj}} + (v_{z,i+k,j})_s \frac{dz}{d\ell} \Big|_{r_{cj}, z_{cj}} \right] Y_{i+k} + \left[(w_{r,i+k,j})_s \frac{dr}{d\ell} \Big|_{r_{cj}, z_{cj}} + (w_{z,i+k,j})_s \frac{dz}{d\ell} \Big|_{r_{cj}, z_{cj}} \right] \frac{dY}{d\ell} \Big|_{i+k} \quad (40)$$

where $(v_{r,i+k,j})_s$, $(v_{z,i+k,j})_s$, $(w_{r,i+k,j})_s$ and $(w_{z,i+k,j})_s$ are the influence functions of Y_{i+k} and $\frac{dY}{d\ell} \Big|_{i+k}$ at the midpoint of segment j

When the values of $Y_{j,av}$ are calculated (using the values of Y_j and $\frac{dY}{d\ell} \Big|_i$ obtained as a result of the first iteration) the splines are passed through these midpoints and two end points of γ -distribution. All subsequent iterations are arranged in the same manner.

Assessment of Accuracy

The accuracy of the solution with polygonal distribution was assessed by direct comparison with a theoretical solution for the flow passing a sphere located inside an infinite surface of revolution formed by a theoretically computed streamline of the translatory flow around the sphere in unbound space (see Figure 2).

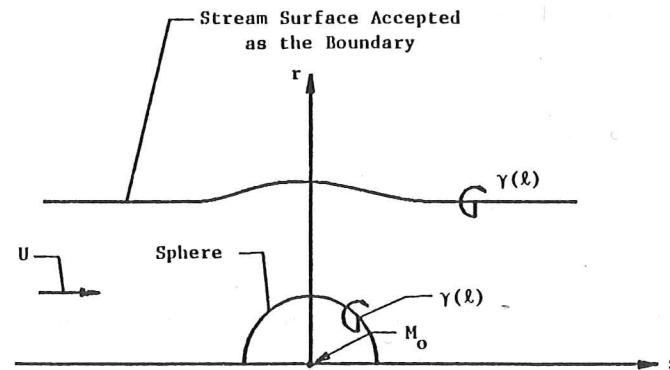


Fig. 2 The fluid passage for the translatory flow around a sphere

The theoretical value for the velocity around a sphere is calculated by the formula [14]:

$$(V_t)_s = 1.5 U \frac{r}{R_s} \quad (40)$$

where U is the velocity of uniform flow in infinity

R_s is radius of the sphere

It is accepted for this comparison that $U = 1.0$ and $R_s = 1.0$. The results of the comparison are shown in Table 1.

The variables in Table 1 are:

- AL Length along the meridional circle forming the sphere
- R and Z Cylindrical coordinates of a point on the meridional circle
- VT Velocity computed by the proposed method

VTE Velocity computed by formula (40)

$$ERV = \left| \frac{VTE - VT}{U} \right| \text{ relative error in velocity computation}$$

As is clear from Table 1 the maximum relative error in computation of the velocity around the sphere is equal to 0.4%. The Table 1 shows

TABLE 1
INFINITE UNIFORM FLOW AROUND SPHERE
(COMPARISON WITH THEORETICAL SOLUTION)

AL	R	Z	VT	VTE	ERV
.01571	.01571	-.99988	.02348	.02356	.00008
.04712	.04711	-.99889	.07034	.07066	.00031
.07854	.07846	-.99692	.11713	.11769	.00056
.10996	.10973	-.99396	.16378	.16460	.00082
.14137	.14090	-.99002	.21025	.21135	.00110
.17279	.17193	-.98511	.25647	.25789	.00142
.20420	.20279	-.97922	.30243	.30418	.00175
.23562	.23345	-.97237	.34807	.35016	.00209
.26704	.26387	-.96456	.39338	.39580	.00242
.29845	.29404	-.95579	.43831	.44105	.00274
.32987	.32392	-.94609	.48283	.48587	.00304
.36128	.35347	-.93544	.52689	.53020	.00331
.39270	.38268	-.92388	.57047	.57402	.00354
.42412	.41151	-.91140	.61352	.61726	.00374
.45553	.43994	-.89803	.65601	.65990	.00389
.48695	.46793	-.88377	.69788	.70188	.00400
.51836	.49546	-.86863	.73911	.74318	.00407
.54978	.52250	-.85264	.77965	.78373	.00409
.58119	.54902	-.83581	.81946	.82352	.00406
.61261	.57501	-.81815	.85850	.86249	.00399
.64403	.60042	-.79968	.89673	.90061	.00388
.67544	.62524	-.78043	.93412	.93785	.00373
.70686	.64945	-.76041	.97062	.97416	.00354
.73827	.67301	-.73963	1.00619	1.00950	.00331
.76969	.69591	-.71813	1.04080	1.04385	.00305
.80111	.71813	-.69591	1.07441	1.07717	.00276
.83252	.73963	-.67301	1.10698	1.10943	.00245
.86394	.76041	-.64945	1.13848	1.14059	.00211
.89535	.78043	-.62524	1.16888	1.17063	.00175
.92677	.79968	-.60042	1.19813	1.19951	.00137
.95819	.81815	-.57501	1.22622	1.22720	.00098
.98960	.83581	-.54902	1.25310	1.25369	.00059
1.02102	.85264	-.52250	1.27875	1.27894	.00019
1.05243	.86863	-.49546	1.30313	1.30292	.00021
1.08385	.88377	-.46793	1.32623	1.32563	.00061
1.11527	.89803	-.43994	1.34801	1.34702	.00100
1.14668	.91140	-.41151	1.36846	1.36708	.00138
1.17810	.92388	-.38268	1.38754	1.38580	.00174
1.20951	.93544	-.35347	1.40524	1.40314	.00209
1.24093	.94609	-.32392	1.42153	1.41910	.00242
1.27235	.95579	-.29404	1.43640	1.43366	.00273
1.30376	.96456	-.26387	1.44983	1.44681	.00302
1.33518	.97237	-.23345	1.46181	1.45853	.00328
1.36659	.97922	-.20279	1.47231	1.46881	.00351
1.39801	.98511	-.17193	1.48134	1.47764	.00371
1.42942	.99002	-.14090	1.48888	1.48501	.00387
1.46084	.99396	-.10973	1.49493	1.49092	.00401
1.49226	.99692	-.07846	1.49946	1.49535	.00411
1.52367	.99889	-.04711	1.50249	1.49831	.00418
1.55509	.99988	-.01571	1.50401	1.49979	.00422

the comparison only for $-1 \leq Z \leq 0$, since for $0 \leq Z \leq 1$ the errors of the computations are the same due to symmetry.

CONCLUSION

The application of the method of singularities to the solution of the axisymmetric problem demonstrated high accuracy in velocity computation even in the case of a polygonal γ -distribution and a conical approximation of the elements forming the boundary. It shows that this technique can be successfully applied to the determination of the axisymmetric flow when it is used as part of the three-dimensional design of the turbo-machine runner. This three-dimensional design is based on a superposition of axisymmetric flow in the fluid passages with the flows produced by the system of the vortices and sources/sinks associated with the blades. High accuracy in computation of each component becomes very important for the achievement of acceptable accuracy for the entire solution.

REFERENCES

1. Martensen, E., "The Calculation of Pressure Distribution on a Cascade of Thick Airfoils by Means of Fredholm Integral Equations of the Second Kind", NASA TTF-702, 1971.
2. Gokhman, A., "The Calculation of a Planar Cascade of Hydrofoils Revolving with Constant Angular Velocity", *Gidromashinostroenie*, No. 2, 1959, pp. 14-19 (Russ.).
3. Gokhman, A., "The Calculation of a Straight Cascade of Thick Hydrofoils by the Method of Singularities with an Angle of Attack", *Energomashinostroenie*, No. 1, 1961, pp. 23-38 (Russ.).
4. Gokhman, A., Rao, Y. V. N., "The Field of Velocities from Singularities in a Thin Lamina of Variable Thickness", *Doklady Akademii Nauk S.S.S.R.*, Vol. 164, No. 5, 1965, pp. 997-1000 (Russ.).
5. Keck, H., "Finite Element Analysis of Flows in Hydraulic Turbomachinery", *Escher-Wyss News*, Vol. 1, No. 2, 1980, pp. 92-100.
6. Marsh, "The Through-Flow Analysis of Axial Flow Compressors", AGARD LS No. 39, Nov. 1970, Paris, France.
7. Gallagher, R. H. et al, "Finite Elements in Fluids", Vol. 12, John Wiley & Sons, 1978.
8. Novak, R. A., "Streamline Curvature Computing Procedures for Fluid Flow Problems", ASME Paper 66-WA/GT-3, 1966.
9. Milovich, A. Y., "Theory of Dynamic Interaction of Bodies and Fluid", Moscow, 1955 (Russ.).
10. Ozboya, N., "Vortex Theory of Three-Dimensional Flows with Free Boundaries", Doctoral Dissertation, June 1981, University of Miami, Florida.

11. Gokhman, A., Leitner, J., "Determination of Streamlines on Stream Surface with Discretely Defined Geometry and Velocity Distribution", *Proceedings of the Symposium on Computation of Internal Flows: Methods and Applications*, ASME, February 1984.
12. Kochin, N., "Vector Calculus and Fundamentals of Tensor Calculus", Moscow, 1981 (Russ.).
13. Gradshteyn, I., Ryzhik, I., "Table of Integrals, Series and Products", 2nd ed., Academic Press, 1980, New York.
14. Kochin, N., et al, "Theoretical Hydromechanics" John Wiley & Sons, 1964, New York.

APPENDIX 1

Velocity Components of the Flow Induced by Circular Vortex Filaments

As shown in [9, 10], the velocity components of the flow induced by vortex Γ , forming the single circular filament ($r = r_0$, $z = z_0$) at the point $r = r_c$, $z = z_c$, can be expressed by:

$$[V_r(r_c, z_c)]_s = - \frac{\Gamma r_0 (z_c - z_0)}{4\pi} \int_0^{2\pi} \frac{\sin\theta d\theta}{[R(r_0, z_0, \theta)]^{1.5}} \quad (41)$$

$$[V_z(r_c, z_c)]_s = - \frac{\Gamma r_0}{4\pi} \int_0^{2\pi} \frac{(r_0 - r_c \sin\theta) d\theta}{[R(r_0, z_0, \theta)]^{1.5}} \quad (42)$$

where

$$R(r_0, z_0, \theta) = r_c^2 - 2r_0 r_c \sin\theta + r_0^2 + (z_0 - z_c)^2 \quad (43)$$

Vortex filaments distributed along radial planes. Using (41) and (42) one can write the formulae for the velocity components (at the point $r = r_c$, $z = z_c$), of the flow induced by the circular vortex filaments, of intensity $\gamma(r)$ (with mutual center at the point $r = 0$), distributed along the part $r_1 \leq r \leq r_2$ of the plane $z = z_0$, as:

$$[V_r(r_c, z_c)]_{z_0, r_2} = - \frac{1}{4\pi} \int_{r_1}^{r_2} \int_0^{2\pi} \frac{\gamma(r)(z_c - z_0) \sin\theta r dr d\theta}{[R(r, z_0, \theta)]^{1.5}} \quad (44)$$

$$[V_z(r_c, z_c)]_{z_0, r_2} = - \frac{1}{4\pi} \int_{r_1}^{r_2} \int_0^{2\pi} \frac{\gamma(r)(r - r_c \sin\theta) r dr d\theta}{[R(r, z_0, \theta)]^{1.5}} \quad (45)$$

In other words for $r_2 \rightarrow \infty$ and $\gamma(r) = \gamma_0/r$ (γ_0 is constant) the velocity components are:

$$[V_r(r_c, z_c)]_{z_0} = - \frac{\gamma_0 (z_c - z_0)}{4\pi} \int_{r_1}^{\infty} \int_0^{2\pi} \frac{\sin\theta r dr d\theta}{[R(r, z_0, \theta)]^{1.5}} \quad (46)$$

$$[V_z(r_c, z_c)]_{z_0} = - \frac{\gamma_0}{4\pi} \int_{r_1}^{\infty} \int_0^{2\pi} \frac{(r - r_c \sin\theta) r dr d\theta}{[R(r, z_0, \theta)]^{1.5}} \quad (47)$$

Changing the order of integration in (46) and (47) and integrating with respect to r one obtains the following formula:

$$[V_r(r_c, z_c)]_{z_0} = - \frac{\gamma_0 (z_c - z_0)}{4\pi} \int_0^{2\pi} \frac{\sin\theta}{P(z_0, \theta)} \times \left[1 - \frac{r_1 - r_c \sin\theta}{[R(r_1, z_0, \theta)]^{0.5}} \right] d\theta \quad (48)$$

where

$$P(z_0, \theta) = (z_c - z_0)^2 + r_c^2 \cos^2\theta \quad (49)$$

$$[V_z(r_c, z_c)]_{z_0} = - \frac{\gamma_0}{4\pi} \int_0^{2\pi} \frac{d\theta}{[R(r_1, z_0, \theta)]^{0.5}} \quad (50)$$

In order to investigate the asymptotic behavior of V_r and V_z when $r_c \rightarrow \infty$ one can apply the binomial theorem to the function $[R(r_1, z_0, \theta)]^{-0.5}$ in formula (48) and (49) (since in this case $r_c \gg r_1$ and $r_c \gg z_c - z_0$) so:

$$[R(r_1, z_0, \theta)]^{-0.5} = \frac{1}{r_c} \left[1 + \frac{r_1}{r_c} \sin\theta - \frac{1}{2} \frac{r_1^2}{r_c^2} + \frac{(z_c - z_0)^2}{2r_c^2} + \frac{3}{2} \frac{r_1^2}{r_c^2} \sin^2\theta + O\left(\frac{1}{r_c^3}\right) \right] \quad (51)$$

$$r_c \gg r_1$$

$$r_c \gg z_c - z_0$$

Substituting (51) into (48) and (50) and integrating one obtains that:

$$[V_r(r_c, z_c)]_{z_0} = \frac{\gamma_0}{2r_c} \left[\pm \sqrt{1 + \lambda^2} + \lambda + O\left(\frac{1}{r_c}\right) \right] \quad (52)$$

$$r_c \gg r_1$$

$$r_c \gg z_c - z_0$$

where

$$\lambda = \frac{z_c - z_0}{r_c}$$

- is for $z_c > z_0$ ($\lambda > 0$)

+ is for $z_c < z_0$ ($\lambda < 0$)

and

$$[V_z(r_c, z_c)]_{z_0} = - \frac{\gamma_0}{2r_c} \left[1 + O\left(\frac{1}{r_c}\right) \right] \quad (53)$$

$$r_c \gg r_1$$

$$r_c \gg z_c - z_0$$

Now using (52) and (53) one can write the formulae for velocity components of the flow induced by the vortices γ_0/r distributed along plane $z = z_0$ and the vortices $-\gamma_0/r$ distributed along plane $z = z_0 + H$ (for $r_c \gg r_1$, $r_c \gg z_c - z_0$, $r_c \gg z_c - z_0 - H$):

for $z_0 \leq z_c \leq z_0 + H$

$$[V_r(r_c, z_c)]_{z_0, z_0+H} = - \frac{\gamma_0}{r_c} \left[1 + O\left(\frac{1}{r_c}\right) \right] \quad (54)$$

for $z_c < z_0$, or for $z_c > z_0 + H$

$$[V_r(r_c, z_c)]_{z_0, z_0+H} = \frac{\gamma_0}{r_c} O\left(\frac{1}{r_c}\right) \quad (55)$$

and for any z_c

$$[V_z(r_c, z_c)]_{z_0, z_0+H} = \frac{\gamma_0}{2r_c} O\left(\frac{1}{r_c}\right) \quad (56)$$

It is easy to see from (54) and (55) that

$$\lim_{r_c \rightarrow \infty} \frac{[V_r(r_c, z_c)]_{z_0, z_0+H}}{-\frac{\gamma_0}{r_c}} = 1 \quad (57)$$

$r_c \rightarrow \infty$ ($z_0 \leq z_c \leq z_0 + H$)

$$\lim_{r_c \rightarrow \infty} \frac{[V_r(r_c, z_c)]_{z_0, z_0+H}}{-\frac{y_0}{r_c}} = 0 \quad (58)$$

$$r_c \rightarrow \infty \quad (z_c < z_0 \text{ or } z_c > z_0 + H)$$

and

$$\lim_{r_c \rightarrow \infty} \frac{[V_z(r_c, z_c)]_{z_0, z_0+H}}{-\frac{y_0}{r_c}} = 0 \quad (59)$$

$$r_c \rightarrow \infty$$

Also it can be proved that the expressions (57), (58) and (59) are valid for any γ -distribution of the following kind:

$$\gamma(r) = \frac{y_0}{r} [1 + \varepsilon(r)]$$

$$\text{where } \lim_{r \rightarrow \infty} \varepsilon(r) = 0$$

Vortex filaments distributed along the cylinder. Using (41) and (42) one can write the formulae for the velocity components (at the point $r = r_c, z = z_c$), of the flow induced by the circular vortex filaments, of intensity $\gamma(z)$ distributed along the part $z_1 \leq z \leq z_2$ of the cylinder $r = r_0$, as:

$$[v_r]_{r_0, z_1, z_2} = -\frac{1}{4\pi} \int_{z_1}^{z_2} \int_0^{2\pi} \frac{\gamma(z)(z_c - z)r_0 \sin\theta d\theta dz}{[R(r_0, z, \theta)]^{1.5}} \quad (60)$$

$$[v_z]_{r_0, z_1, z_2} = -\frac{1}{4\pi} \int_{z_1}^{z_2} \int_0^{2\pi} \frac{\gamma(z)(r_0 - r_c \sin\theta)r_0 dz d\theta}{[R(r_0, z, \theta)]^{1.5}} \quad (61)$$

Also for $\gamma = y_0$ and $z_2 \rightarrow \infty$ (or $z_1 \rightarrow -\infty$) after integration with respect to z (see [10]) the velocity components, for the semifinite cylinders ($r = r_0$) covered with constant vortex rings y_0 , are:

$$[V_r]_{r_0} = \pm \frac{y_0}{2\pi} \int_{\pi/2}^{3\pi/2} \frac{r_0 \sin\theta d\theta}{[R(r_0, z_0, \theta)]^{0.5}} \quad (62)$$

$$[V_z]_{r_0} = \frac{y_0}{2\pi} \int_{\pi/2}^{3\pi/2} \frac{(r_0 - r_c \sin\theta)r_0}{Q(r_0, \theta)} \times [-1 \pm \frac{z_e - z_c}{[R(r_0, z_e, \theta)]^{0.5}}] d\theta \quad (63)$$

where + is for cylinder $z_e \leq z < \infty$

- is for cylinder $-\infty < z \leq z_e$

and

$$Q(r_0, \theta) = r_c^2 - 2r_c r_0 \sin\theta + r_0^2 \quad (64)$$

Using formulae (62), (63), (64) and results obtained in [10] one can prove that for a semi-infinite annulus, ($r_{ci} \leq r \leq r_{co}$) covered with $-y_0$ along the outer cylinder and with y_0 along the inner cylinder, the following formulae apply:

$$\lim [V_r]_{r_{ci}, r_{co}} = 0 \quad (65)$$

$$z \rightarrow \pm \infty$$

$$\lim [V_z]_{r_{ci}, r_{co}} = y_0 \quad (66)$$

$$z \rightarrow \pm \infty \quad [r_{ci} \leq r \leq r_{co}]$$

$$\lim [V_z]_{r_{ci}, r_{co}} = 0 \quad (67)$$

$$z \rightarrow \pm \infty \quad [0 < r < r_{ci} \text{ or } r > r_{co}]$$

In the formulae (65), (66) and (67) the sign + corresponds to annulus the ($z_e \leq z < \infty$) and the sign - corresponds to the annulus ($-\infty < z \leq z_e$).

Additionally it can be proved that the expressions (65), (66) and (67) are valid for any γ -distribution of the following kind:

$$\gamma = y_0 (1 + \varepsilon(z))$$

$$\text{where } \lim_{z \rightarrow \infty} \varepsilon(z) = 0$$

Vortex filaments distributed along an arbitrary surface of revolution. An arbitrary surface of revolution can be described in parametric form by two equations for its meridional line:

$$\begin{aligned} r &= r(\ell) \\ z &= z(\ell) \end{aligned} \quad (68)$$

where ℓ is the length along the meridional line of the surface

The velocity components at a point (r_c, z_c) induced by the circle vortex filaments intensity $\gamma(\ell)$ along the surface (68) for $\ell_1 < \ell < \ell_2$ are:

$$[V_r]_s = - \int_{\ell_1}^{\ell_2} \int_0^{2\pi} \frac{\gamma(\ell)(z_c - z) \sin\theta r d\theta d\ell}{4\pi [R(r, z, \theta)]^{1.5}} \quad (69)$$

$$[V_z]_s = - \int_{\ell_1}^{\ell_2} \int_0^{2\pi} \frac{\gamma(\ell)(r - r_c \sin\theta) r d\theta d\ell}{4\pi [R(r, z, \theta)]^{1.5}} \quad (70)$$

The equation (68) can be successfully approximated using splining technique [11]. The curve (68) is divided into segments and on each segment it is defined by Hermite interpolant polynomials (H-coefficients are defined in (38)).

$$r^i(\ell) = r_i H_{01} + r_{i+1} H_{11} + \Delta \ell_i \left(\frac{dr}{d\ell} \Big|_i H_{02} + \frac{dr}{d\ell} \Big|_{i+1} H_{12} \right) \quad (71)$$

$$z^i(\ell) = z_i H_{01} + z_{i+1} H_{11} + \Delta \ell_i \left(\frac{dz}{d\ell} \Big|_i H_{02} + \frac{dz}{d\ell} \Big|_{i+1} H_{12} \right) \quad (72)$$

Therefore, since the function $\gamma(\ell)$ can be expressed by a Hermite interpolant polynomial on each segment i of curve (68) as:

$$\gamma^i(\ell) = \gamma_i H_{01} + \gamma_{i+1} H_{11} + \Delta \ell_i \left(\frac{d\gamma}{d\ell} \Big|_i H_{02} + \frac{d\gamma}{d\ell} \Big|_{i+1} H_{12} \right) \quad (73)$$

the integration with respect to ℓ can be carried out in formulae (69) and (70).

After a substitution of (71), (72) and (73) into the formulae (69) and (70) one obtains the following expressions for the velocity components at the point (r_c, z_c) induced by the vortices $\gamma^i(\ell)$ distributed along segment i of the surface (68):

$$V_r^i = \gamma_i [F_{01}]_r + \gamma_{i+1} [F_{11}]_r + \frac{d\gamma}{d\ell} \Big|_i [F_{02}]_r + \frac{d\gamma}{d\ell} \Big|_{i+1} [F_{12}]_r \quad (74)$$

$$V_z^i = \gamma_i [F_{01}]_z + \gamma_{i+1} [F_{11}]_z + \frac{d\gamma}{d\ell} \Big|_i [F_{02}]_z + \frac{d\gamma}{d\ell} \Big|_{i+1} [F_{12}]_z \quad (75)$$

Each function F in the formulae (74) and (75) has the following form:

$$F = \int_0^{2\pi} \int_0^1 \frac{[\sum_{n=0}^9 \lambda^n \phi_n(\theta)] \Delta \ell_i d\lambda}{4\pi [\sum_{n=0}^9 \lambda^n \psi_n(\theta)]^{1.5}} \quad (76)$$

It is clear that integrals of this type cannot be taken analytically neither with respect to λ nor θ . In the case of the conical approximation of surface element i :

$$r^i(\lambda) = r_i(1-\lambda) + r_{i+1}\lambda \quad (77)$$

$$z^i(\lambda) = z_i(1-\lambda) + z_{i+1}\lambda \quad (78)$$

and

$$\Delta \ell_i^2 = (r_{i+1} - r_i)^2 + (z_{i+1} - z_i)^2 \quad (79)$$

The denominator in the formula (76) becomes simpler and integration with respect to λ can be achieved.

Indeed, using (43), (77), (78) and (79), one obtains:

$$R(r, z, \theta) = A_2 \lambda^2 + A_1 \lambda + A_0 \quad (80)$$

where

$$A_0 = r_c^2 - 2r_c r_i \sin\theta + r_i^2 + (z_c - z_i)^2$$

$$A_1 = 2[(r_{i+1} - r_i)(r_i - r_c \sin\theta) + (z_{i+1} - z_i)(z_i - z_c)]$$

$$A_2 = \Delta \ell_i^2$$

Consequently in view of (80) the expressions for coefficients F in the formulae (74) and (75) in case of a conical segment have this form:

$$F = \int_0^{2\pi} \int_0^1 \frac{[\sum_{n=0}^9 \lambda^n \phi_n(\theta)] \Delta \ell_i d\lambda}{4\pi (A_2 \lambda^2 + A_1 \lambda + A_0)^{1.5}} \quad (81)$$

Integration with respect to λ can be easily carried in the formula (81) using the table integral 2.263 on Page 82 in [13]. The actual formulae obtained as a result of this integration are rather cumbersome and do not fit the format of the present paper.

Now consider the point (r_c, z_c) which belongs the conical element i , or (using (77) and (78)):

$$r_c = r_i + \lambda_c (r_{i+1} - r_i) \quad (82)$$

$$z_c = z_i + \lambda_c (z_{i+1} - z_i)$$

where

$$0 \leq \lambda_c \leq 1$$

Substituting (82) into (80) one obtains, for $\theta = \pi/2$, that:

$$R(r, z, \theta) = \Delta \ell_i (\lambda^2 - 2\lambda \lambda_c + \lambda_c^2) \quad (83)$$

It is clear that for $\lambda = \lambda_c$, $R(r, z, \theta) = 0$ and that the integral (81) is improper. Generally speaking the integrals (69) and (70) are improper if the point (r_c, z_c) belongs to the surface of revolution (68), since $[R(r, z, \theta)]^{0.5}$ (which is the distance between the points (r, z, θ) and $(r_c, z_c, \pi/2)$) becomes zero when $r = r_c$, $z = z_c$ and $\theta = \pi/2$. It is shown in Appendix 2 how to compute the velocity components V_r and V_z for a point (r_c, z_c) belonging to the surface (68).

Computation of Velocity Components Induced by Vortices Along a Conical Element at a Point Outside the Element

The formulae for the velocity components induced by vortices distributed along a conical element were developed in detail in the doctoral dissertation of Dr. N. Ozboya [10] (the author of the present paper was his graduate adviser). These formulae are based on evident relations for γ -distribution along conical element (these relations were accepted instead of relations (82) and (83) for convenience of derivation):

$$r(s) = c_r + f_r s \quad (84)$$

$$z(s) = c_z + f_z s \quad (85)$$

$$\gamma(s) = c_g + f_g s \quad (86)$$

where s is the distance along segment Δl forming element, with $s = 0$ at the midpoint ($-0.5\Delta l \leq s \leq 0.5\Delta l$)

$c_r = r(0)$, $c_z = z(0)$ and $c_g = \gamma(0)$ are the values of r , z and γ at the middle point of segment

f_r , f_z and f_g are the derivatives of r , z and γ with respect to s along the segment

As follows from (69), (70), (84), (85) and (86):

$$V_r = -\frac{1}{2\pi} \int_{-\frac{\Delta l}{2}}^{\frac{\Delta l}{2}} \sin\theta d\theta \int_{-\frac{\Delta l}{2}}^{\frac{\Delta l}{2}} \frac{A_{r1}s^3 + A_{r2}s^2 + A_{r3}s + A_{r4}}{R^{3/2}} ds \quad (87)$$

$$V_z = -\frac{1}{2\pi} \int_{-\frac{\Delta l}{2}}^{\frac{\Delta l}{2}} d\theta \int_{-\frac{\Delta l}{2}}^{\frac{\Delta l}{2}} \frac{A_{z1}s^3 + A_{z2}s^2 + A_{z3}s + A_{z4}}{R^{3/2}} ds \quad (88)$$

where

$$\begin{aligned} A_{r1} &= -f_z (f_g f_r + h_g c_r) \\ A_{r2} &= f_g f_r (z_c - c_z) - f_z (f_g c_r + f_r c_g) \\ A_{r3} &= (c_g f_r + c_r f_g)(z_c - c_z) - f_z c_r c_g \\ A_{r4} &= c_g c_r (z_c - c_z) \\ A_{z1} &= f_g f_r^2 \\ A_{z2} &= c_g f_r^2 + f_g f_r (2c_r - r_c \sin\theta) \\ A_{z3} &= f_r c_g (2c_r - r_c \sin\theta) + c_r f_g (c_r - r_c \sin\theta) \\ A_{z4} &= c_g c_r (c_r - r_c \sin\theta) \end{aligned}$$

and $R = B_1 s^2 + B_2 s + B_3 \quad (89)$

where

$$\begin{aligned} B_1 &= f_r^2 + f_z^2 = 1 \\ B_2 &= 2f_r(c_r - r_c \sin\theta) + 2f_z(c_z - z_c) \\ B_3 &= r_c^2 - 2r_c c_r \sin\theta + c_r^2 + (c_z - z_c)^2 \end{aligned}$$

The final formulae after integration with respect to s are [13]:

$$V_r = -\frac{1}{2\pi} \int_{-\frac{\Delta l}{2}}^{\frac{\Delta l}{2}} (A_{r1}T_3 + A_{r2}T_2 + A_{r3}T_1 + A_{r4}T_0) \sin\theta d\theta \quad (90)$$

$$V_z = -\frac{1}{2\pi} \int_{-\frac{\Delta l}{2}}^{\frac{\Delta l}{2}} (A_{z1}T_3 + A_{z2}T_2 + A_{z3}T_1 + A_{z4}T_0) d\theta \quad (91)$$

where:

$$\begin{aligned} T_0 &= \frac{2(2s+B_2)}{\Delta R^{1/2}} \\ T_1 &= \frac{2(2B_3+B_2s)}{\Delta R^{1/2}} \\ T_2 &= -\frac{(\Delta-B_2^2)s - 2B_2B_3}{\Delta R^{1/2}} + \ln |2\sqrt{R} + 2s + B_2| \\ T_3 &= \frac{\Delta s^2 + B_2(10B_3 - 3B_2^2)s + B_3(8B_3 - 3B_2^2)}{\Delta R^{1/2}} - \frac{3B_2}{2} \ln |2\sqrt{R} + 2s + B_2| \\ \Delta &= 4B_3 - B_2^2 \end{aligned}$$

The integrals (90) and (91) have to be integrated numerically with respect to θ . It is not difficult for the point (r_c, z_c) which does not belong to the conical segment. The case of (r_c, z_c) being the midpoint of the straight segment forming the conical element is evaluated in next section of this Appendix.

Computation of Velocity Components Induced by Vortices Along a Conical Element at the Midpoint of the Segment Forming this Element

It was shown in Appendix 1 that R is equal to zero for the point $r = r_c$, $z = z_c$ and $\theta = \pi/2$ and therefore the functions T_0 , T_1 , T_2 and T_3 in (90) and (91) become infinite. Consequently, in this case the integrals (90) and (91) cannot be taken numerically for the limits $\pi/2$ and $3\pi/2$.

Let:

$$I_r = A_{r1}T_3 + A_{r2}T_2 + A_{r3}T_1 + A_{r4}T_0$$

and

$$I_z = A_{z1}T_3 + A_{z2}T_2 + A_{z3}T_1 + A_{z4}T_0$$

The one can write in this case for $\varepsilon > 0$, that

$$V_r = V_{r1} + V_{r2} \quad (92)$$

$$V_z = V_{z1} + V_{z2} \quad (93)$$

where

$$V_{r1} = -\frac{1}{2\pi} \int_{\frac{\pi}{2} + \varepsilon}^{\frac{\pi}{2}} I_r \sin\theta d\theta$$

$$V_{r2} = -\frac{1}{2\pi} \int_{\frac{\pi}{2}}^{\frac{\pi}{2} + \varepsilon} I_r \sin\theta d\theta$$

$$V_{z1} = -\frac{1}{2\pi} \int_{\frac{\pi}{2} + \varepsilon}^{\frac{\pi}{2}} I_z d\theta$$

$$V_{z2} = -\frac{1}{2\pi} \int_{\frac{\pi}{2}}^{\frac{\pi}{2} + \varepsilon} I_z d\theta$$

It is clear that V_{r2} and V_{z2} can be computed numerically since θ is never equal to $\pi/2$. For the computation of V_{r1} and V_{z1} the function $\sin\theta$ (which is the source of all difficulties in the analytic integration with respect to θ in the formulae (90) and (91)) was written as:

$$\sin\theta = \sin\left(\frac{\pi}{2} + \delta\right) = 1 - \frac{\delta^2}{2} \quad (0 \leq \delta \leq \varepsilon) \quad (94)$$

Using (94) the integrals defining V_{r1} and V_{z1} can be easily taken analytically as follows [10]:

$$V_{r1} = f_g \frac{1}{2\pi} \left[\left(\ln \frac{\Delta l}{c_r} - \ln \varepsilon \right) 2c_r f_z \varepsilon + c_g \frac{1}{2\pi} \left[\left(\ln \frac{\Delta l}{c_r} - \ln \varepsilon - 0.5 \right) 2f_r f_z \varepsilon \right] \right] \quad (95)$$

$$V_{z1} = f_g \frac{1}{2\pi} \left(\ln \varepsilon - \ln \frac{\Delta l}{c_r} \right) 2f_r c_r \varepsilon + c_g \frac{1}{2\pi} \left[f_r^2 - 1 + 2f_r^2 \left(\ln \varepsilon - \ln \frac{\Delta l}{c_r} \right) \right] \varepsilon \quad (96)$$

The formulae (92), (93), (95) and (96) can be used for very accurate computation of V_r and V_z at the

midpoint if one accepts the proper method for the computation of V_{r2} and V_{z2} and proper value for ε . The formula (94) gives a very good accuracy for $\varepsilon \leq 0.05$:

$$\theta_1 = 0.05 + \frac{\pi}{2}$$

$$\sin\theta_1 = 0.998750$$

$$1 - \frac{0.05^2}{2} = 0.998750$$